Colloid and Polymer Science (2020) 298:103–111
https://doi.org/10.1007/s00396-019-04568-5

ORIGINAL CONTRIBUTION

Electrospun PCL-based polyurethane/HA microfibers as drug carrier of dexamethasone with enhanced biodegradability and shape memory performances

Haitao Lv[1] · Dongyan Tang[1] · Zhaojie Sun[1] · Jingru Gao[1] · Xu Yang[1] · Shuyue Jia[1] · Jing Peng[1]

Received: 6 May 2019 / Revised: 18 August 2019 / Accepted: 10 September 2019 / Published online: 4 December 2019

Abstract

Shape memory polymers (SMP) with better biodegradability and better stability have great potential applications in biomedical fields, such as the drug carriers or the tissue engineering scaffolds. In this study, poly(ε-caprolactone)(PCL)-based polyurethane(PU) microfibers were fabricated with the containing of hydroxyapatite(HA) to enhance the biodegradability and to exhibit excellent shape memory performance. The composition, the morphology, the thermal stability, and the mechanical properties of the microfibers were characterized and detected using Fourier transform infrared spectroscopy (FTIR), ^{1}H nuclear magnetic resonance (^{1}HNMR), scanning electron microscopy (SEM), differential scanning calorimetry (DSC). and dynamic mechanical analysis (DMA), etc. And dexamethasone was selected as drug model to investigate the delivery and release behaviors of the carrier of the microfibers. It was revealed that HA enhanced the degradation rate of the shape memory polyurethane (SMPU) fibers, and the fibers could guarantee a sustained long time drug release. The detection on the shape memory performance found that, with the different addition amounts of HA, the composite microfibers of (SMPU) and HA exhibited the different shape memory transition temperature (T_{trans}) values. And with the addition of 3 wt% of HA, the excellent shape recovery ratios of R_r (> 97%) and the shortest recovery time of ~ 6 s could be obtained. With further increase of the amounts of HA, the recovery force and the recovery time were reduced and prolonged, respectively. The obtained results proved that the biodegradable SMPU/HA composite microfibers have more valuable application prospects in biomedical fields.

Keywords Shape memory polyurethane · Biodegradable · Electrospinning · Drug release

Introduction

Shape memory polymers (SMP) are typical kinds of burgeoning intelligent materials that have attracted more and more attention in the past few decades. While such materials undergo the different environmental stimuli, such as chemical [1], electrical [2], and light, magnetic, or thermal triggered shape changes [3, 4], they would have the recovery ability to their initial states from the deformed states to show the shape memory behaviors. As the most extensively investigated shape memory materials among the various SMP [5], thermally induced SMP have been widely studied, and focused on accumulating their potential applications in biomedical devices [6, 7], including cardiovascular stents, sutures, drug-eluting stents [8], clot removal devices [9], and tissue engineering [10, 11].

Polyurethanes as one of excellent SMP have been drawing increasing attention in practices due to their abilities to recover large deformation, characteristics of lower cost, ease in processing, desirable biocompatibility [12], high resistance to organic solvents and aqueous solutions, and adjusted transition temperatures with the changing of surroundings and body temperatures, etc. [4]. For shape memory polyurethane (SMPU), their shape memory performances could be tailored by using special functionalized soft segments and hard segments into the polymers [13]. Until now, more and more attention was drawn to the soft segments of poly(ε-caprolactone)(PCL) for the synthesis of thermal induced SMPU [14], and on their bio-related applications, due to the excellent biodegradability, biocompatibility, and elasticity of

✉ Dongyan Tang
dytang@hit.edu.cn

[1] School of Chemistry and Chemical Engineering, Harbin Institute of Technology, Harbin 150001, China

thus synthesized PU [15, 16]. Moreover, the glass transition temperature (T_g) and the melting temperature (T_m) of PCL could be easily tuned by altering its chain length or by copolymerization with other polymer segments [17]. Nevertheless, the still unsatisfied modulus owing to the higher elastics and the still need to be improved biocompatibility of PCL-based SMPU both restrict the medical applications to some extents. So the composites with higher modulus components, and the fabrications to some special morphologies with SMPU, are of great significance.

As major parts of mineral component in bone [18], hydroxyapatite (HA) nanocrystals have been widely used as bone fillers and the implant materials for many years, due to its excellent bioactivity, biocompatibility, and osteoconductivity [19, 20]. And one of just a few bioactive materials used means it can support bone repairs and regeneration more effectively [20]. Thus, the addition of HA into systems could not only improve the biocompatibility and bioactivity, but also could be beneficial to achieve enhanced mechanical properties and the shape memory effect [20–23]. And by the fabrication into non-woven textile mats, oriented fibrous bundles, and even three-dimensional structured scaffolds [24, 25], electrospinning has been remarkably recognized as one of the most attractive nanotechnologies to produce microfibers/nanofibers with high porosity and specific surface area that are suitable for a variety of biomedical applications [26, 27], such as tissue engineering, controlled drug delivery, sensing, separations, and filtration and catalysis [28]. It has been illustrated that the high specific surface area of the micro/nano scale SMPU fibers would be more sensitive to external stimuli, and have rapid response ability. So biodegradable SMPU fibers could effectively enhance the tissue repair and the regeneration efficacy [29].

So in this work, a novel SMPU/HA biomimetic composite nanofibers with enhanced biological performance and improved shape memory properties for the potential use in biomedical fields were designed. And dexamethasone (DEX), a synthetic glucocorticoid compound [30], and one of the ideal bone formation accelerator with good stability [31, 32], was selected as drug model to investigate its controllable release behavior within the carrier in an attempt to avoid the producing of toxic effects, the inducing of bone loss and osteoporosis effectively, owing to the relative large concentration of DEX [7, 33].

Materials and methods

Materials

Poly(ε-caprolactone) diol (PCL, Mn = 2000), HA nanoparticles (< 200-nm particle size), and DEX were purchased from Aldrich Co., Ltd. Isophorone diisocyanate (IPDI) were purchased from Alfa (USA). Stannous octoate ($SnOct_2$) was purchased from A Damas Beta. 1,4-Butanediol (BDO), N,N-dimethylformamide (DMF), and ethanol were purchased from Aladdin Chemical Reagent (Shanghai, China). They were all of analytical grades and used directly without further purification.

Synthesis of shape memory PCL-polyurethane

SMPU with IPDI:PCL:BDO in a molar ratio of 2.5:1.0:1.5 was synthesized by step addition polymerization, according to the following procedure. PCL diol was dried overnight in vacuum oven at 45 °C. The prepolymer was synthesized at 75 °C by reacting with IPDI and PCL diol for 2 h under nitrogen with mechanical stirring. Then the chain extension reaction of the prepolymers was carried out by dropping BDO to dissolve in DMF and 0.1–0.5 wt% of $SnOct_2$, as catalyst, was added into the prepolymers. The reaction temperature was maintained to below to 60 °C for another 2 h. DMF was added into the reactor occasionally when necessary to reduce the viscosity of the reactant mixture. The viscous solution was precipitated in methanol and then dried in vacuum oven at 50 °C until a constant weight was reached.

Preparation of SMPU/HA and SMPU/HA/DEX nanocomposites

To prepare SMPU/HA and SMPU/HA/DEX spinning dope, a two-step method was utilized for the dispersion of HA nanoparticles into polymer solution. First, HA nanoparticles and DEX were dispersed in DMF and sonicated at room temperature. Then SMPU was dissolved in DMF and added into HA/DMF and HA/DEX/DMF system under stirring overnight to achieve a homogeneous solution. The proportion of HA in SMPU/HA mixture was 1, 3, and 5 wt% and DEX was dispersed in SMPU/HA solution with the concentration of 0.5 mg/g.

Electrospinning of SMPU fibers and composite fibers with HA and EDX

The above-prepared spinning dope was loaded in a 5-ml syringe with a metal needle of 0.55-mm inner diameter. The flow rate of solution was set to be 0.15 ml/h and the applied voltage was 14 kV. The tip-to-collector distance was 22 cm, and a grounded aluminum sheet was used as collector. The schematic diagram was shown in Fig. 1. After electrospinning, the formed nanofibers were dried in vacuum for over 2 days to remove the potential residual solvents.

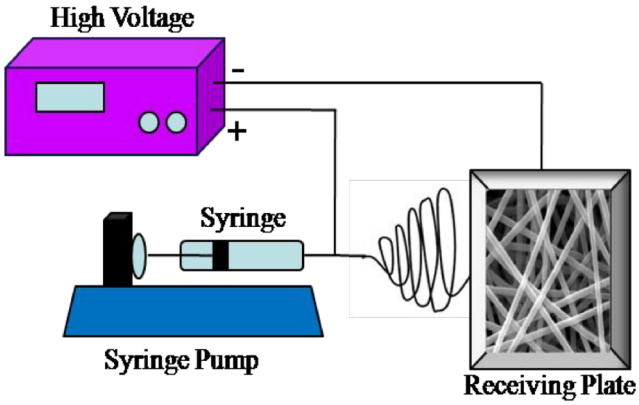

Fig. 1 Schematic diagram of horizontal set up of electrospinning apparatus

Analysis and characterization

Morphology of the fibers was analyzed with a field emission scanning electron microscope (Helios Nanolab600i, FEI, USA) at an accelerating voltage of 10 kV, after sputter coating with platinum. The average diameter of the fibers was determined by using Image J software. Functional groups presented in the particles were determined by using Fourier transform infrared (FTIR) spectroscopic analysis on Avatar 360 (Thermo Nicolet, USA) over a range of 400–4000 cm^{-1} at a resolution of 8 cm^{-1}. Thermal properties of HA powder and the electrospun fibers were measured by differential scanning calorimetry (DSC) on a TA instrument (SDTQ600, USA) operating at 10 °C/min heating rate. Nitrogen flushing was used to supply protective atmosphere. ^1H NMR spectra were recorded at room temperature with a Bruker spectrometer operating at 300 MHz using deuterated chloroform ($CDCl_3$) as solvent. Chemical shifts (*d*) were given in parts per million using tetramethylsilane as an internal reference.

Shape memory behaviors detection

Dynamic mechanical measurements of the electrospun composite fibers were carried out on a dynamic mechanical analyzer (Q800 DMA, TA Instruments) in tensile mode. The analyses were conducted using a preload force of 0.01 N, a shock range of 15 μm, and a frequency of 1 Hz. The shape memory (SM) behaviors of all the samples were evaluated by the following procedure. Typically, the strip, which was 5.5 mm in width and 0.15 mm in thickness, was heated to 45 °C (where the T_m was obtained from the DSC) and kept under an isothermal condition for 5 min to obtain an original shape (ε_o). Then it was stretched from 0 to 0.1 MPa at a rate of 0.01 MPa min^{-1} to obtain a deformed shape (ε_d). Then the deformed sample was fixed (ε_f) when it decreased to 0 °C at a rate of 3 °C min^{-1}. Then the stress of the samples was released to 0 MPa at a rate of 0.05 MPa min^{-1}. After that, the shape memory behavior was performed when heated to 45 °C again at a rate of 3 °C min^{-1} to obtain a recovery shape (ε_r). The shape recovery ratio (R_r) and shape fixed ratio (R_f) were defined and calculated as follows:

$$R_f(\%) = \frac{\varepsilon_f}{\varepsilon_d} \times 100\% \quad (1)$$

$$Rr(\%) = \frac{\varepsilon_d - \varepsilon_r}{\varepsilon_d - \varepsilon_o} \times 100\% \quad (2)$$

All the calculations of the shape fixation ratios and the shape recovery ratios were based on the second cycle of stress-controlled testing.

The macroscopic SM evaluations of pure SMPU and SMPU/HA composite fibers were carried out and recorded by a digital camera. The samples with the same temporary shape and the same thickness of 0.15 cm were deformed at 45 °C, stored at 0 °C to maintain their temporary shape and then recovered their permanent shape at 45 °C.

In vitro degradation and drug release experiments

The samples of SMPU nanofibers were placed in phosphate buffered saline (PBS) solution (pH of 7.4) in an incubator shaker at 37° C and 100 rpm for periods of time. For every 3 days, the buffer solution was replaced from the samples. The degraded fibers were rinsed carefully with ultrapure water and then was air dried in vacuum, finally the fibers was weighed. The degradation rate was calculated from the dried weight before and after the degradation via the following formula (3):

$$Weight\ \ Loss(\%) = \frac{W_o - W_d}{W_o} \times 100\% \quad (3)$$

where W_0 was the original weight before the degradation and W_d was the dry weight after the degradation.

Dexamethasone (10 mg) was weighed and transferred to a 100-mL flask containing 100 mL of 0.1 mol/L HCl. Then 1 mL of the solution was transferred to another 100-mL flask to obtain solutions with different concentrations of 10, 20, 30, 40, and 50 μg/mL. The absorbance was taken on double beam UV spectrophotometer using λ_{max} of 243 nm. The absorbance values were plotted against the concentration (μg/mL) to obtain the standard calibration curve.

Drug release experiments were carried out in 10.0 mL PBS solution with 25-mL sample vial and the solution was placed in an incubator shaker (37° C, 100 rpm). SMPU nanofibers containing dexamethasone were then immersed in PBS and placed in an incubator shaker at 37 °C and 200 rpm. At particular time intervals, 2-mL samples were removed and the drug concentration was determined by spectrophotometer at the wavenumber of 243.5 nm. The samples were replaced with fresh buffer in order to keep the constant volume of the release medium.

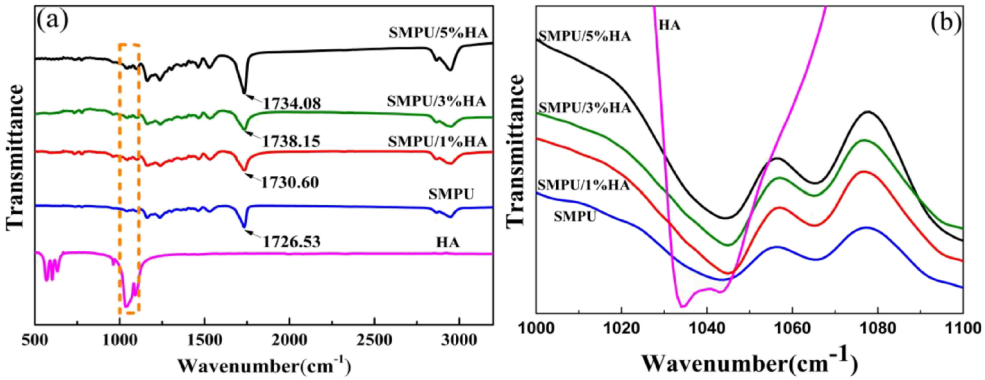

Fig. 2 FTIR spectra of **a** SMPU microfibers, HA nanoparticles, and SMPU/HA composite microfibers. **b** Magnified FTIR spectra of (**a**) at the range of wave numbers from 1000 to 1100 cm^{-1}

Results and discussion

Characterization of SMPU microfibers and SMPU/HA composite microfibers

FTIR spectra of SMPU microfibers, HA nanoparticles, and SMPU/HA composite fibers were shown in Fig. 2. From Fig. 2 a, we can find that the presence of C=O (ester) stretching vibration at 1726 cm^{-1} corresponded to ester linkages, and that at 1093 cm^{-1} to C–O stretching. The unchanging of the spectra of SMPU/HA with the increase of HA content indicated the non-influence of HA on the functional groups of SMPU. However, the alteration of C=O stretching vibration peak of SMPU from 1726 to 1738 cm^{-1} for SMPU/HA fibers might be due to the formation of hydrogen bonds between –OH group in HA and –C=O group in SMPU. And in Fig. 2 b, the characteristic peak of phosphate group (PO_4^{3-}) in HA appeared at 1034 cm^{-1}, and similarly, the location for the peak of PO_4^{3-} group changed to 1043 cm^{-1} because of the formation of hydrogen bonding between –C=O group in SMPU and P–OH group in HA [26].

Thermally triggered SMPU usually makes use of a thermal transition such as T_g or T_m for the recovery, thus it is necessary to further identify the transition temperature with SMPU/HA composite fibers. Figure 3 a and b showed the DSC heating curves of SMPU/HA composite fibers with different proportions of HA. It can be seen that T_m of SMPU fibers was 36.7 °C. And as the HA ratios increased from 1 to 5% in SMPU/HA composite fibers, the temperatures of T_m would rise to 45.6 °C. The results showed that the composite fibers exhibited a tendency of possessing a relative higher T_m with the increase of HA content in the composite fibers, which was well known as the effect of the filler content on the chain segment movement of the matrices. This signified that HA particles might provide nucleation sites for SMPU chain segments and would be able to crystallize at a higher temperature when SMPU/HA composites were cooled down from amorphous state [13, 34].

^{1}H NMR spectra of the obtained SMPU were shown in Fig. 4. The signal peaks of a at δ of 4.5–4.8 ppm were assigned to amide proton of urethane linkage (–CO–NH–). The methylene protons near carboxyl group (–CH_2–O–CO–) appeared at δ of 4.05 ppm (peak b), and the linear methylene protons (–CH_2–CO–O–) appeared at δ of 2.31 ppm (peak c). Additionally, peak at δ of 3.88 ppm (peak d) was attributed to methylene protons from ether group (–O–CH_2–), and peaks at δ of 2.88 ppm (peak e) were attributed to –CH_2– between –NH–COO– and hexatomic ring [35, 36].

Morphology of SMPU/HA composite fibers

As shown in Figure 5(a–d), the fiber diameter of SMPU increased from 690 ± 120 to 780 ± 150 nm for SMPU/1%HA, while decreased to 730 ± 140 nm for SMPU/3%HA and further decreased to 630 ± 120 nm after the addition of relative higher amount of HA (Fig. 5(e)). And compared with the

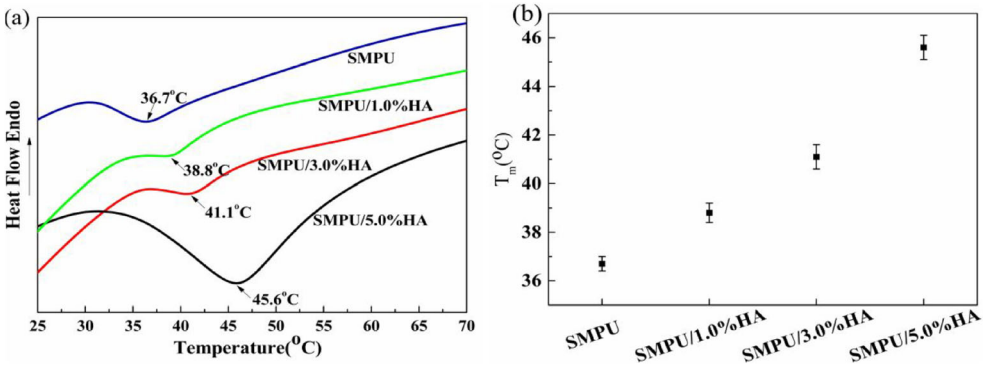

Fig. 3 DSC curves of the electrospun SMPU/HA composite fibers with different incorporation amounts of HA. **b** The derived T_m values of the electrospun SMPU/HA composite fibers from (**a**)

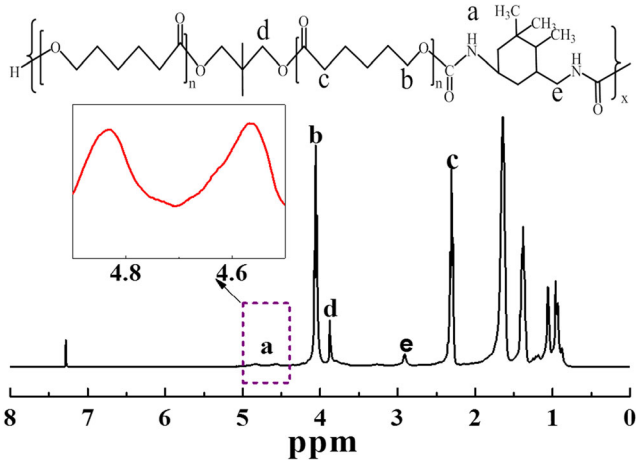

Fig. 4 ^{1}H NMR spectrum with characteristic chemical shifts and chemical structure of SMPU matrix

glossy morphology of SMPU microfibers (as shown in Fig. 5(a)), a few tiny nanoparticle knots were found on the surface of SMPU/3%HA fiber (blue circle) (as shown in Fig. 5(c)), whereas SMPU/5%HA fiber emerged a few more agglomerates that were uniformly distributed on the surface of fibers (as shown in Fig. 5(d)). So SEM micrographs revealed that the incorporation with HA into SMPU microfibers did not alter the uniform and glossy fibrous morphology of SMPU fibers significantly. And the appearance of the agglomerates might be due to the inter-particle van der Waals interactions and the formation of hydrogen bonding between hydroxyl groups on the surface of HA nanoparticles [28]. And for all the electrospun fibrous mats, the similar pore sizes (~ 4 μm) might be owing to the alignment of the formed fibers by the injected fibers mostly and thus the variation of the sizes was only within a small range [29].

Shape memory properties of SMPU and SMPU/HA composite fibers

Performance in tensile or modulus and the shape stability with the change of the surroundings might be the essential requirements for the applicable ability of biomaterials. Figure 6 a showed the representative tensile stress−strain curves and the derived tensile properties of SMPU fibers with the different addition ratios of HA. By using DMA test, the mechanical properties of SMPU fibers and SMPU/HA composite fibers were measured at physiological temperature (~ 37 °C).

Incorporation with HA into SMPU fibers had effects on the tensile strength and Young's modulus of the composites. Compared with SMPU fibers, SMPU/HA fibers containing 1% and 3% HA showed strengthened tensile properties due to the well-known reinforcing effect of HA and the formation of the hydrogen bonding interactions between the functional groups of HA and SMPU (as shown in Fig. 2). And the tensile strength of the composite fibers of SMPU/1%HA and SMPU/3%HA had increased doubled and tripled values approximately, respectively. However, when the amount of HA loading reached to a critical volume fraction of 5%, the HA nanoparticles can easily be agglomerated because of its high surface active energies. The aggregation of HA (as shown in Fig. 5(d)) introduced the disruption and discontinuities among

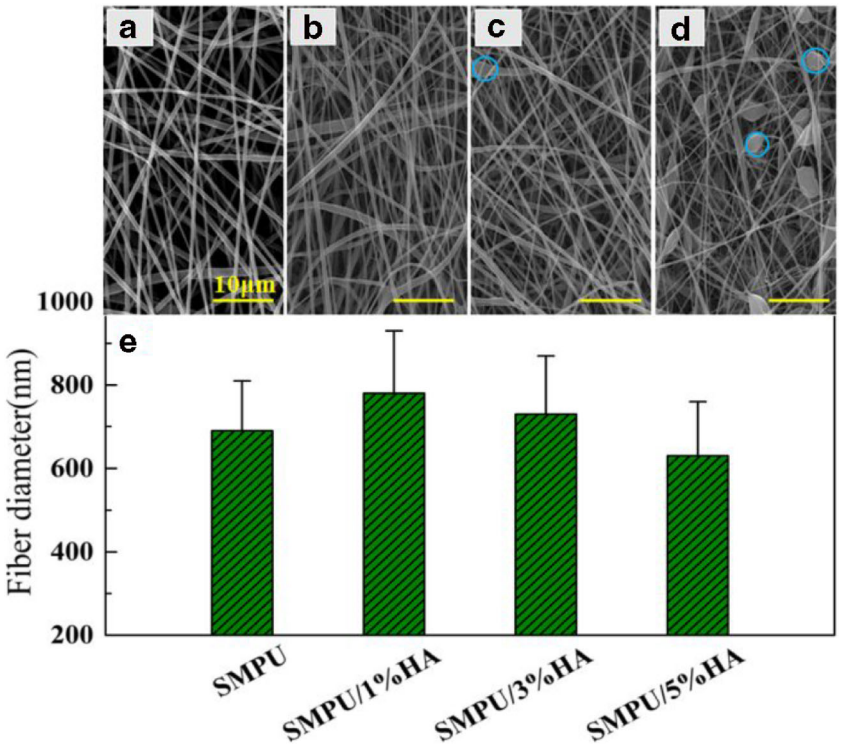

Fig. 5 (a–d) SEM micrographs of the electrospun fibers (a) of SMPU fibers, (b) SMPU/1%HA composite fibers, (c) SMPU/3%HA composite fibers, and (d) SMPU/5% HA composite fibers. (e) The comparison of the diameters of SMPU/HA composite fibers with varied loading amount of HA

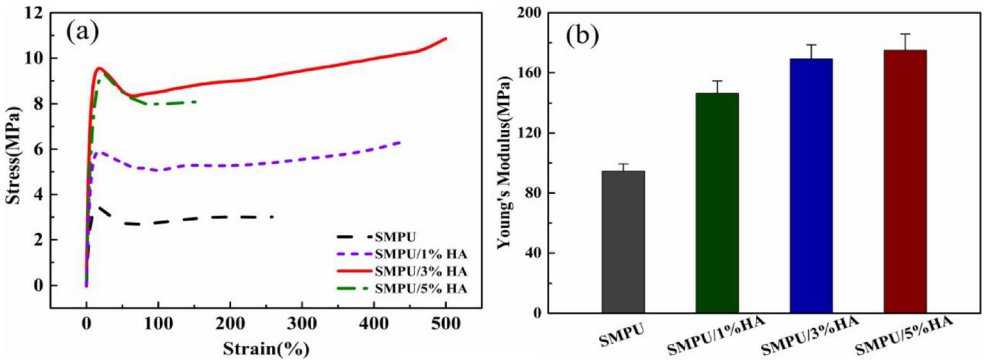

Fig. 6 Strain-stress curves (**a**) and Young's modulus (**b**) of the electrospun SMPU/HA composite fibers tested at 37 °C

the formed fiber chains, and that could directly accelerate the breakage of the microfibers during the tensile tests. Interestingly, the variation in Young's modulus showed a positive correlation with the added concentration of HA (as shown in Fig. 6b), owing to the role of the filler of HA and thus enhanced the fibers' strength [20]. From the above, SMPU/3%HA microfibers had relative excellent performance both in the tensile performance and in Young's modulus.

According to the DMA detection results, SMPU/3%HA fibers with relative excellent performance both in the tensile performance and in Young's modulus were chosen for the further tests of the shape memory behaviors. Figure 7 showed a visual comparison of the shape recovery capacity of SMPU fibers and SMPU/3%HA composite fibers. The permanent (initial) shape of the fibers was in a strip, the shape recovery from a temporary shape of straight spiral can be completed in a short time for about 6 s upon the deformed spiral of a temperature of 40 °C, which was in the acceptable range of shape recovery temperatures. The intuitive results showed that HA played a key role in the reinforcement in the shape memory ability.

To further investigate the effects of HA contents in composite fibers to the shape memory behaviors quantitatively, a well-established cyclic thermo-mechanical tests were applied and the four-step thermo-mechanical cycling method was carried out by using DMA method (as shown in Fig. 8).

In the case of SMPU fibers (Fig. 8a), a temperate strain of 110% was deformed, the loading stress reached 0.1 MPa in the initial stress–strain curve and the shape recovery ratio calculated according to the final strain-temperature curve was 84%. As a control, the shape memory (SM) cycle of SMPU/3%HA composite fibers was investigated (Fig. 8b), it was deformed a stain of 190% and the final strain-temperature curve was promoted to 97%.

Moreover, the effect of temperatures on the shape memory performances of SMPU fibers and SMPU/HA composite fibers was explored. All the investigated samples (30 × 5.5 × 0.15 mm) were incubated at 45 °C for 5 min and then were elongated. Then the deformed samples were fixed by staying at − 20 °C for 30 min. Thus the shape memory performances at different temperatures were observed and the shape memory ability was quantified by formula (1). From Fig. 9, compared with the most unrecovery of the deformed samples at 25 °C, while all the temporary shapes were placed at 37 °C (which was close to the human physiological temperature), the R_r could reach up to 83.2% for SMPU fibers and 93.6%

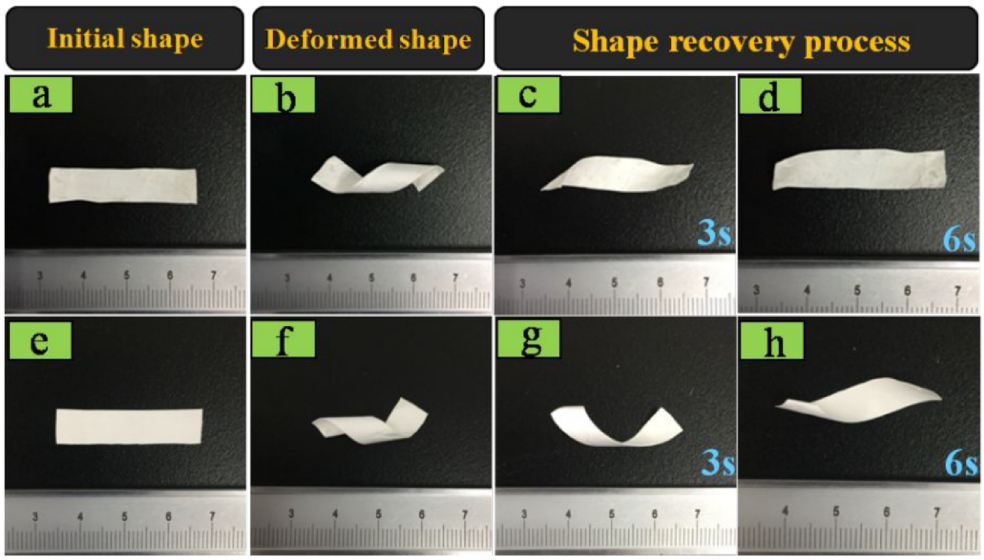

Fig. 7 The optical photos of the shape recovery of SMPU/3%HA fibers (a–d) and SMPU fibers (e–h)

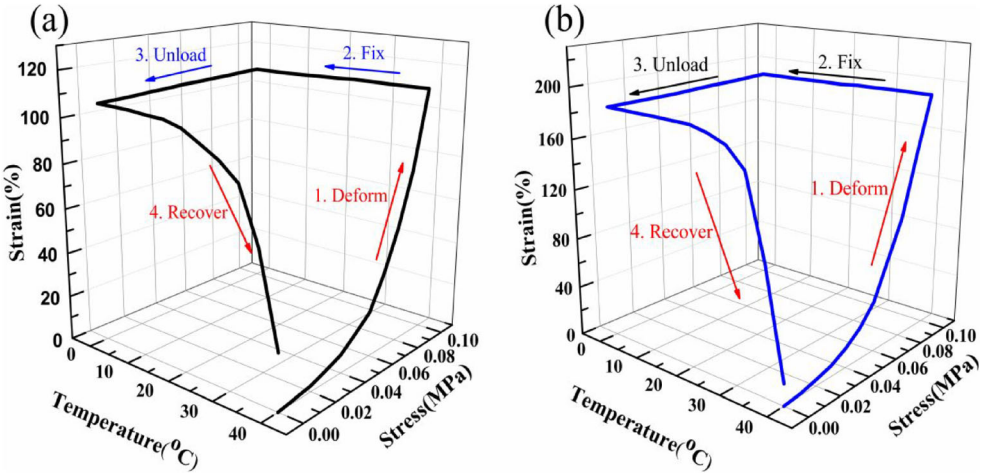

Fig. 8 Stress–temperature–strain data of the shape memory cycles for **a** SMPU fibers and **b** SMPU/3%HA composite fibers

for SMPU/3%HA composite fibers. And further, relative excellent shape recovery performances were observed at 45 °C; for that, the R_r values reached up to 91.3%, 97.3%, and 96.5% for SMPU/1%HA, SMPU/3%HA, and SMPU/5%HA composite fibers, respectively. Thus, the incorporation of HA had a positive impact on the shape memory properties of SMPU, and the result was in good accordance with the results reported by Du et al [18].

Degradation performances of SMPU fibers and SMPU/HA fibers and drug release behaviors with EDX

Biodegradable polymers have attracted more and more attention in tissue engineering and in other medical application fields, because of the hydrolysis ability of the relative high molecular weight chains (and the high molecular weight chains would guarantee relative excellent performance required for applications) into nontoxic oligomers to human body.

The biodegradability performance of SMPU fibers and SMPU/HA composite fibers with HA content of 1, 3, and 5% were studied. And the weight loss percentage ratios of the composites in vitro degradation were exemplified in Fig. 10. After 10 weeks of degradation, the weight loss rates of SMPU fibers was about 12.1%, and the degradation rates grew with the increased contents of HA in the composite fibers. The weight loss of SMPU/1%HA, SMPU/3%HA, and SMPU/5%HA was 14.5%, 17.1%, and 19.1% after degradation for 10 weeks, respectively. The slower degradation rate of SMPU compared with that of SMPU/HA composite fibers might be the relative higher crystallization degree of SMPU than that of SMPU/HA composites [8, 30, 37].

DEX was selected as drug model to investigate the release behavior from the carrier of the electrospun mats in PBS at 37 °C, and the cumulative release of DEX was shown in Fig. 11. All the mats exhibited slower sustained release of DEX over

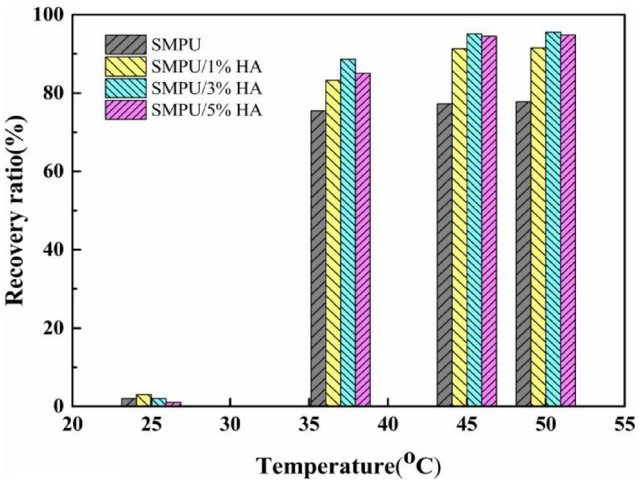

Fig. 9 The shape memory ratios of SMPU fibers and SMPU/HA composite fibers with the changing of temperatures

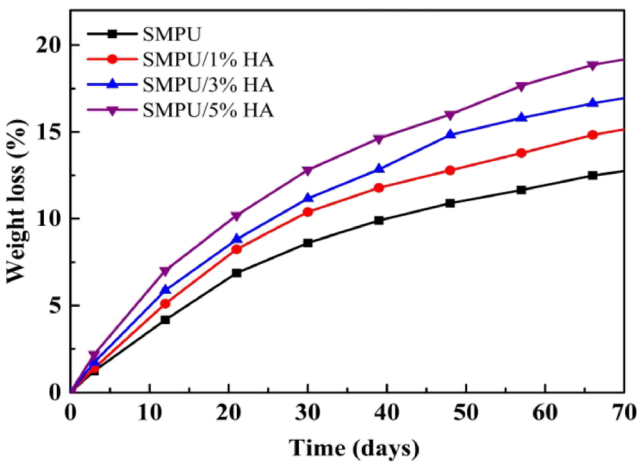

Fig. 10 The biodegradable performance of SMPU fibers and SMPU/HA composite fibers represented by the weight loss during in vitro release

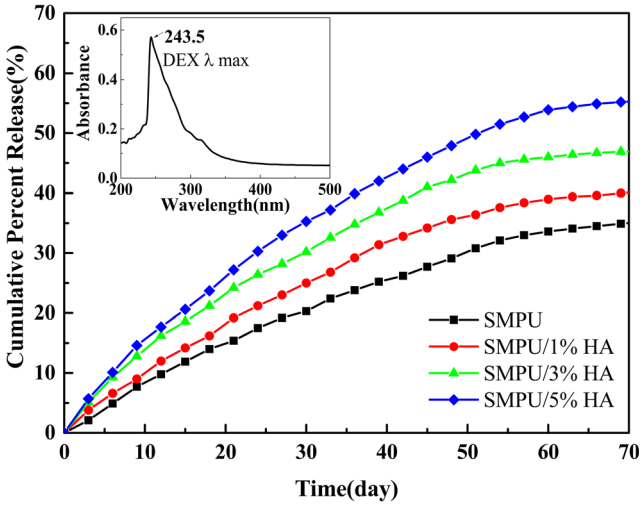

Fig. 11 Cumulative release profile of DEX from SMPU and SMPU/HA electrospun fibers with DEX (Inset: the UV-vis spectra of DEX)

10 weeks, and importantly, no initial burst release could be observed, which would guarantee a long time sustained release of DEX [32, 38].

While in case of SMPU/HA mats, the release showed growing trends with the increasing content of HA in SMPU fibers. This indicated that the release was mainly depended on the degradation rates, which meant the long chains of polymer could be hydrolyzed into oligomers with the release of drug molecules. And thus the introduction of HA into the fibers enhanced the biodegradability and the controlled release of drugs to the electrospun microfibers effectively.

Conclusion

The enhanced biodegradability and shape memory performance of SMPU microfibers were fabricated by the incorporation with HA into the system. The composite fibers exhibited better controlled drug release with EDX as drug model for its potential use in medical fields. Varying loading ratios of HA in the composite fibers affected the shape memory transition temperatures and the shape memory recovery ratios. And SMPU with 3 wt% of HA exhibited relative excellent R_r of > 97% and recovery ability with the shortest recovery time of about 6 s, owing to its probable appropriate interactions with SMPU and relative excellent mechanical properties in tensile and modulus values. So further increase in the content of HA would reduce the recovery force and prolong the recovery time. The obtained results proved that the biodegradable SMPU/HA composite fibers have application prospects in bio-medical fields.

Funding information The studies were financially supported by the Excellent Academic Leaders Foundation of Harbin, China (No. 2014RFXXJ017) and the Open Project of State Key Laboratory of Urban Water Resource and Environment, Harbin Institute of Technology (No. QA201610-02).

Compliance with ethical standards

Conflict of interest The authors declare that they have no conflict of interest.

References

1. Chen H, Li Y, Liu Y, Gong T, Wang L, Zhou S (2014) Highly pH-sensitive polyurethane exhibiting shape memory and drug release. Polym Chem 5:5168–5174
2. Wu Y, Wang L, Guo B, Shao Y, Ma PX (2016) Electroactive biodegradable polyurethane significantly enhanced Schwann cells myelin gene expression and neurotrophin secretion for peripheral nerve tissue engineering. Biomaterials 87:18–31
3. Behl M, Razzaq MY, Lendlein A (2010) Multifunctional shape-memory polymers. Adv Mater 22:3388–3410
4. Behl M, Lendlein A (2007) Shape-memory polymers. Mater Today 10:20–28
5. Pieczyska EA, Maj M, Kowalczyk-Gajewska K, Staszczak M, Gradys A, Majewski M, Cristea M, Tobushi H, Hayashi S (2015) Thermomechanical properties of polyurethane shape memory polymer–experiment and modelling. Smart Mater Struct 24:045043
6. Serrano MC, Ameer GA (2012) Recent insights into the biomedical applications of shape-memory polymers. Macromol Biosci 12:1156–1171
7. Wong Y, Kong J, Widjaja LK, Venkatraman SS (2014) Biomedical applications of shape-memory polymers: how practically useful are they? Sci China Chem 57:476–489
8. Kashif M, Yun B-m, Lee K-S, Chang Y-W (2016) Biodegradable shape-memory poly(ε-caprolactone)/polyhedral oligomeric silsequioxane nanocomposites: sustained drug release and hydrolytic degradation. Mater Lett 166:125–128
9. Huang WM, Song CL, Fu YQ, Wang CC, Zhao Y, Purnawali H, Lu HB, Tang C, Ding Z, Zhang JL (2013) Shaping tissue with shape memory materials. Adv Drug Deliv Rev 65:515–535
10. Baudis S, Behl M, Lendlein A (2014) Smart polymers for biomedical applications. Macromol Chem Phys 215:2399–2402
11. Gu L, Cui B, Wu Q-Y, Yu H (2016) Bio-based polyurethanes with shape memory behavior at body temperature: effect of different chain extenders. RSC Adv. 6:17888–17895
12. Mather PT, Luo X, Rousseau IA (2009) Shape memory polymer research. Ann Rev Mater Res 39:445–471
13. Zhang Y, Wang C, Pei X, Wang Q, Wang T (2010) Shape memory polyurethanes containing azo exhibiting photoisomerization function. J Mat Chem 20:9976–9981
14. Yang CS, Wu HC, Sun JS, Hsiao HM, Wang TW (2013) Thermo-induced shape-memory PEG-PCL copolymer as a dual-drug-eluting biodegradable stent. ACS Appl Mater Interfaces 5:10985–10994
15. Feng Y, Zhang S, Wang H, Zhao H, Lu J, Guo J, Behl M, Lendlein A (2011) Drug release from biodegradable polyesterurethanes with shape-memory effect. J Control Release 152(Suppl 1):e20–e21
16. Zhang SF, Feng YK, Zhang L, Guo JT, Xu YS (2010) Biodegradable Polyesterurethane Networks for Controlled Release of Aspirin. J Appl Polym Sci 116:861–867
17. Nail LN, Zhang D, Reinhard JL, Grunlan MA (2015) Fabrication of a bioactive, PCL-based "Self-fitting" Shape Memory Polymer Scaffold. J Vis Exp 104:52981–52988

18. Du K, Gan Z (2014) Shape memory behaviour of HA-g-PDLLA nanocomposites prepared via in situ polymerization. J Mat Chem B 2:3340–3348
19. Kutikov AB, Reyer KA, Song J (2014) Shape Memory performance of thermoplastic amphiphilic triblock copolymer poly(D,L-lactic acid-co-ethylene glycol-co-D,L-lactic acid) (PELA)/hydroxyapatite composites. Macromol Chem Phys 215:2482–2490
20. Bao M, Wang X, Yuan H, Lou X, Zhao Q, Zhang Y (2016) HAp incorporated ultrafine polymeric fibers with shape memory effect for potential use in bone screw hole healing. J Mater Chem B 4: 5308–5320
21. Wong TW, Wahit MU, Abdul Kadir MR, Soheilmoghaddam M, Balakrishnan H (2014) A novel poly(xylitol-co-dodecanedioate)/ hydroxyapatite composite with shape-memory behaviour. Mater Lett 126:105–108
22. Reit R, Lund B, Voit W (2014) Shape memory polymer–inorganic hybrid nanocomposites. Adv Polym Sci 267:313–350
23. Zou H, Weder C, Simon YC (2015) Shape-memory polyurethane nanocomposites with single layer or bilayer oleic acid-coated Fe3O4nanoparticles. Macromol. Mater. Eng 300:885–892
24. Zhuo H, Hu J, Chen S (2008) Electrospun polyurethane nanofibres having shape memory effect. Mater Lett 62:2074–2076
25. Hunley MT, Long TE (2008) Electrospinning functional nanoscale fibers: a perspective for the future. Polym Int 57:385–389
26. Zhang JN, Ma YM, Zhang JJ, Xu D, Yang QL, Guan JG, Cao XY, Jiang L (2011) Microfiber SMPU film affords quicker shape recovery than the bulk one. Mater Lett 65:3639–3642
27. Guo F, Wang N, Wang L, Hou L, Ma L, Liu J, Chen Y, Fan B, Zhao Y (2015) An electrospun strong PCL/PU composite vascular graft with mechanical anisotropy and cyclic stability. J Mater Chem A 3: 4782–4787
28. Hager MD, Bode S, Weber C, Schubert US (2015) Shape memory polymers: Past, present and future developments. Prog Polym Sci 49-50:3–33
29. Chen H, Cao X, Zhang J, Zhang J, Ma Y, Shi G, Ke Y, Tong D, Jiang L (2012) Electrospun shape memory film with reversible fibrous structure. J Mat Chem 22:22387–22391
30. Gandhimathi C (2015) Controlled release of dexamethasone in PCL/silk fibroin/ascorbic acid nanoparticles for the initiation of adipose derived stem cells into osteogenesis. J Drug Metab Toxicol 5:177–183
31. Su Y, Su Q, Liu W, Lim M, Venugopal JR, Mo X, Ramakrishna S, Al-Deyab SS, El-Newehy M (2012) Controlled release of bone morphogenetic protein 2 and dexamethasone loaded in core-shell PLLACL-collagen fibers for use in bone tissue engineering. Acta Biomater 8:763–771
32. Costa PF, Puga AM, Diaz-Gomez L, Concheiro A, Busch DH, Alvarez-Lorenzo C (2015) Additive manufacturing of scaffolds with dexamethasone controlled release for enhanced bone regeneration. Int J Pharm 496:541–550
33. Neffe AT, Hanh BD, Steuer S, Lendlein A (2009) Polymer networks combining controlled drug release, biodegradation, and shape memory capability. Adv Mater 21:3394–3398
34. Ping P, Wang W, Chen X, Jing X (2007) The influence of hard-segments on two-phase structure and shape memory properties of PCL-based segmented polyurethanes. J Polym Sci Pt B-Polym Phys 45:557–570
35. Cui J, Kratz K, Heuchel M, Hiebl B, Lendlein A (2011) Mechanically active scaffolds from radio-opaque shape-memory polymer-based composites. Polym Adv Technol 22:180–189
36. Lakatos C, Czifrak K, Papp R, Karger-Kocsis J, Zsuga M, Keki S (2016) Segmented linear shape memory polyurethanes with thermoreversible Diels-Alder coupling: Effects of polycaprolactone molecular weight and diisocyanate type. Express Polym Lett 10: 324–336
37. Fujihara K, Kotaki M, Ramakrishna S (2005) Guided bone regeneration membrane made of polycaprolactone/ calcium carbonate composite nano-fibers. Biomaterials 26:4139–4147
38. Fratoddi I, Venditti I, Cametti C, Palocci C, Chronopoulou L, Marino M, Acconcia F, Russo MV (2012) Functional polymeric nanoparticles for dexamethasone loading and release. Colloids Surf B: Biointerfaces 93:59–66